机器人的CP-nets优化类人轨迹规划

刘兆伟[1,2], 仲兆琳[2], 王　磊[2], 李　珂[1†]

(1. 山东大学 控制科学与工程学院, 山东 济南 250061; 2. 烟台大学 计算机与控制工程学院, 山东 烟台 264005)

摘要: 机器人移动轨迹按照人的手臂来模拟是提高机器人安全性和人机交互能力的有效方法; 特别是针对机器人抓取路径不唯一的场合, 类人行为对于人机系统表现更加自然. 此前, 通常利用Kinect等设备, 基于人工神经网络和K近邻算法等智能算法对类人轨迹进行规划, 但无法获得未采样过的最优轨迹. 本文基于CP-nets采用偏好模型研究类人运动轨迹, 然后将该模型应用于机器人控制, 在没有采样的情况下, 也可得到最优的类人轨迹. 实验结果表明, 基于CP-nets的类人规划轨迹具有较高的效率和舒适性, 符合人的运动特征.

关键词: 机器控制; 人机系统; CP-nets; 轨迹

引用格式: 刘兆伟, 仲兆琳, 王磊, 等. 机器人的CP-nets优化类人轨迹规划. 控制理论与应用, 2018, 35(12): 1772 – 1778

中图分类号: TP242.2　　　**文献标识码:** A

Optimal human-like trajectory planning of CP-nets for robot

LIU Zhao-wei[1,2], ZHONG Zhao-lin[2], WANG Lei[2], LI Ke[1†]

(1. School of control science and engineering, Shandong University, Jinan Shandong 250061, China;
2. School of computer science and control engineering, Yantai University, Yantai Shandong 264005, China)

Abstract: Robot moving trajectory simulated with human arm and wrist is an effective method to improve the safety of the robot and the ability of human-robot interaction. Especially, the reaching path for robot hand grasping is not unique. Human-like system is known as more understandable and natural for human-robot interaction. The planning of human-like trajectory were presented based on intelligent algorithm like as artificial neural network and the K-nearest neighbors algorithm by using the Kinect or other equipment, but they cannot learn the optimal trajectory which not been sampled. In this paper, a preference model is adopted to study the trajectory of human-like movement based on CP-nets. Then the model is applied on the robot control to obtain the optimal human-like trajectory even it not been sampled. The results showed that the planned trajectory has high efficiency and comfort with human like movement characteristics.

Key words: robot control; human-machine system; CP-nets; trajectory

Citation: LIU Zhaowei, ZHONG Zhaolin, WANG Lei, et al. Optimal human-like trajectory planning of CP-nets for robot. *Control Theory & Applications*, 2018, 35(12): 1772 – 1778

1 Introduction

With the development of industrialization and informatization, the robot technology has become an important symbol of the era of technology innovation. Currently, robots have been extensively used in manufacturing, military, medical, security, service and other fields[1–2]. Compared with the traditional industry, such as automobile assembly and loading and unloading, many works can't complete separately by human beings or robots, like as invasive surgery and precision instrument processing, which put forward a higher requirement for trajectory planning of robot[3–4].

Recently, research about the trajectory control of robots has made great achievement. The relationship of the rotation angles of manipulator motion and the rotation angle of gestures have now been presented. And the theory has been applied to the control of the robot arm[5–6]. This work provides support for the use of human motion control robots. In addition, the trajectory optimization and simulation of the robot have also aquired certain achievements. The time-optimal trajectory with non-linear kinematic constraints of six joint robots by using the improved particle swarm optimization[7–8]. Using the GL graphics library can well simulate the trajectory of the robot[9], the trajectory of robot by simulation experiment can be observed. In recent research, a trajectory planning system based on an artificial neural network architecture trained on human

actions has been realized[10], it usually can provide a human-like trajectory for robot.

At present, the trajectory of the end effector of the industrial robot is mainly pre-determined by the use of the teaching device and complicated control systems[11–12]. The operation is complex. This paper collects the trajectory of human wrist by Kinect[13–16] equipment and studies and obtains the control method of robots trajectory by using of CP-nets[17], making the robots arm can imitate the human motion strategy and reproduce the human wrist trajectory. The contributions of this paper are mainly divided into the following three aspects.

1) Data acquisition based on Kinect and related kit. Based on the computer vision, we obtain the video data-stream information by Kinect, processing the image by Kinect SDK, segmenting the dynamic attitude of wrists from the video signal and exacting the three-dimensional location data. Consequently, the human wrist trajectory is obtained.

2) Trajectory planning with CP-nets. Based on the CP-net model, the trajectory of the wrist joint is studied, and the preference relation of the human hand movement is obtained, and a control method to realize the humanoid trajectory is presented.

3) Application in robots. Sending the human-like trajectory of robot end effector which planed by trajectory planning algorithm to the robots as the control order, the robots can be controlled.

The remainder of this paper is organized as follows: in Section 2, we put forward a realization method to collect trajectory of human wrist joint; in Section 3, we adopt the CP-nets to figure out the human-like trajectory; in Section 4, a series of experiments and discussions is introduced. Finally, we conclude the whole paper with opportunities for future work in Section 5.

2 Data acquisition

In this section, we use the optical device to track human joints positions and realize data-collection. To acquire the hand trajectory online, it is required to design a human arm model and construct a wrist motion trajectory data set. We also explain how to by using of Kinect equipment collect wrist motion trajectory[15–16, 18].

2.1 Arm model

In this subsection, we abstract arm into the model which consists of shaft and linkage[15], as shown in Fig. 1.

Degrees of $q_1 \sim q_6$ in Fig. 1 represent the 6 degrees of freedom of arm from the shoulder to the wrist (device can be rotated as the perpendicular bisector of the bottom of the cylinder is axis). The q_1 degree represents the shoulder, which drives the lifting and landing of the whole arm. The q_2 degree represents the upper arm, and it can rotate itself. The q_3 degree represents the elbow joint and it can drive the arm swing. The q_4 degree represents the lower arm and has the same degree of freedom as degree q_2. The q_5 and q_6 degree represents the wrist joint which can achieve the swinging back and forth, up and down of hands[18–19]. The model has similar structure characteristics as six axis robots like as KUKA KR210.
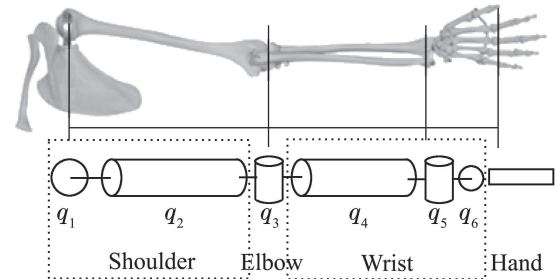

Fig. 1 Human arm equivalent joint model

With the above model, the wrist is corresponding to the end effector of robots and takes the trajectory of human wrist with sampling, and carries out the planning of the trajectory of the robots end effector[19].

2.2 Kinematics solution of robot

The kinematics analysis of the robot is the foundation of the study of the robot trajectory, and it is the precondition of the trajectory planning[20–23]. The trajectory planning of the six degree of freedom chain manipulator can be carried out in two kinds of space, namely: joint space and cartesian space[24–25]. Among them, the joint space trajectory planning is the controlled variable of motion or angle rotation of each joint direct planning, this model has some identities like as small amount of computation, easy to control, easy adjustment of robot pose, but this method is difficult to determine the trajectory of the end effector of the end of each link coupling. In this paper, we discuss the trajectory planning problem of six axis robot, mainly for planning the trajectory of the end effector of the robot, so it is carried out in cartesian space[26–27].

In the kinematics solution of the robot, the Denavit-HartenBerg representation is an intuitionistic and widely used method[28–29]. Kinematic modeling of the robot by D–H method is shown in Fig. 2.
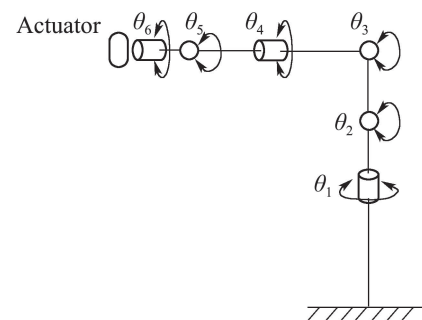

Fig. 2 D–H model

According to the established D–H model, the transformation matrix T_n^{n-1} of the n connecting rod relative to the $n-1$ connecting rod can be determined. The matrix needs to satisfy the following formula:

$$T_n^{n-1} = \begin{bmatrix} \cos\theta_n & -\sin\theta_n & 0 & \alpha_{n-1} \\ \sin\theta_n\cos\alpha_{n-1} & \cos\theta_n\cos\alpha_{n-1} & -\sin\alpha_{n-1} & -\sin\alpha_{n-1}d_n \\ \sin\theta_n\cos\alpha_{n-1} & \cos\theta_n\cos\alpha_{n-1} & \cos\alpha_{n-1} & \cos\alpha_{n-1}d_n \\ 0 & 0 & 0 & 1 \end{bmatrix}. \tag{1}$$

Then the coordinate system of the robot terminal actuator is expressed as

$$T_{\text{end}} = T_1^0 T_2^1 T_3^2 T_4^3 T_5^4 T_6^5. \tag{2}$$

The rotation angle of all joints can be obtained with a series of matrix operations.

2.3 The design and acquisition of trajectory data

A subject (male, right-handed, 24 years old, 175 cm tall) was instructed to perform reaching motions in a natural manner, from a starting point to a target position. For the same target point, the model can take any way to the point and score the comfort of each track. In the course of movement, the model remains the shoulder joint in stationary when performing all the grasping motion and keeps the wrist in a uniform motion. All movements started at zero velocity and ended at the target at zero velocity. Every grasping motion remains three or four seconds to fully collect space data of wrist.

This paper uses Kinect (microsoft corporation) to collect the trajectory of human wrist. The Kinect can obtain the color image and depth image, and its accuracy depends on the distance between the camera and the measurement object. When the distance is about 2∼3 meters, the precision is highest, with 1.5∼3 cm error[14]. In this paper, the trajectory of wrist is abstracted as a series of discrete Cartesian product position, which begins from the starting coordinate, after multiple passing points, ends with terminal coordinate. The coordinate system of Kinect camera is right-handed helix[13]. Kinect camera is right in the coordinate origin. The positive axis of X extends left (from the view of Kinect), the positive axis of Y extends upward, the Z axis points the direction that Kinect camera faces[13–14].

In this paper, we convert the joint coordinates by converting mode of Cartesian product coordinate system, and set up the wrist coordinates. We select the coordinate of right wrist in a fall naturally state as the origin of reference coordinate system to convert coordinates.

When the model arm falls naturally, the coordinate of right hand in Kinect coordinate system is $D_0(x_0, y_0, z_0)$, with getting the coordinate in the movement of right wrist continually, $D_1(x_1, y_1, z_1)$, $D_2(x_2, y_2, z_2)$, $D_3(x_3, y_3, z_3), \cdots, D_n(x_n, y_n, z_n)$. Set the starting point of wrist joint as the origin, and represents these points as follows.

$$d_1 = D_1(x_1, y_1, z_1) - D_0(x_0, y_0, z_0), \tag{3}$$

$$d_2 = D_2(x_2, y_2, z_2) - D_0(x_0, y_0, z_0), \tag{4}$$

$$\vdots$$

$$d_n = D_n(x_n, y_n, z_n) - D_0(x_0, y_0, z_0). \tag{5}$$

Let $D_0(x_0, y_0, z_0) = (0, 0, 0)$, then the trajectory formed by $D_0(x_0, y_0, z_0), d_1, d_2, \cdots, d_n$ is the trajectory of wrist joint.

By using Kinect to collect wrist trajectory, we need to make the following preparations in advance:
1) Configure and initialize the cameras.
2) Set collection trigger mode.
3) Set the image collection frame.
4) Open skeleton tracking function.

Figure 3 is the schematic diagram of wrist joint motion trajectory. (a) is data collecting at the starting point, (b) and (c) are the middle process, (d) is the data collecting at the target point.
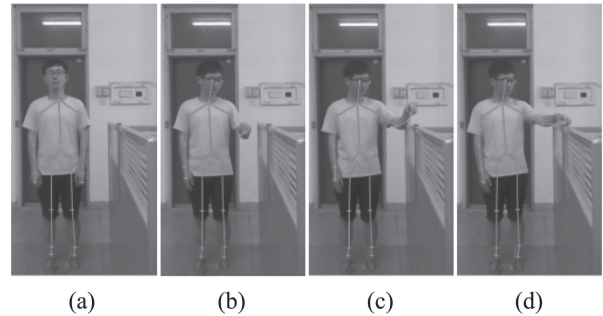

| (a) | (b) | (c) | (d) |

Fig. 3 Schematic diagram of wrist joint motion trajectory

During the collecting process of wrist trajectory, there will be noise points because of the wrist shaking and Kinect system factors. At present, there are many schemes for dealing with trajectory noise, like different filtering algorithms and machine learning. This section uses a relatively simple mean filtering algorithm for trajectory preprocessing. The trajectory collection algorithm is shown in Algorithm 1.

Algorithm 1 (Hand trajectory collection algorithm)
Input: Grasping motion
Start color camera and depth camera
Trigger the device and start recording data
For (time = 0, time < 5, time++)
    do retrieve the framework and checks whether
         skeletons are tracked
      If the human skeleton is detected
        do check the skeleton data from the depth
            element.

Extract and store wrist space coo-rdinates
Else continue
End for
Return: extract the consecutive multiple wrist joints space coordinates, and draw the trajectory
Output: The trajectory of human wrist

The mean filtering is a nonlinear signal processing technology based on the order statistical theory. It can effectively suppress the noise[20–21]. The basic principle of mean filtering is that the value of a point in a digital image or sequence is replaced by the average value of all points in a neighborhood, thus removes noises. The mathematical expression of mean filtering is shown in the following formula:

$$g(x,y) = \frac{\sum f(i,j)}{\text{num}(f)}, \ f(i,j) \in \Omega. \quad (6)$$

In the formula 6, $g(x,y)$ is the coordinate of the output point, Ω represents the point $g(x,y)$'s neighborhood of fixed radius, $f(i,j)$ represents the coordinates of other points in this neighborhood, $\text{num}(f)$ is the number of the points in the neighborhood.

The trajectory which collected by the mean filtering is much more smooth, and removes all of the noise almost in the data set. After the above work, we can get the wrist movement trajectory data set. The trajectory of the wrist collected in the above is continuous, in order to facilitate the calculation, we do the following action to collect the data. We put the new data set D of each trajectory uniform 11 points. It contains a starting point, a target point and nine passing points[18–19]. The trajectory of a collection of multiple hand movements as shown in Fig. 4. The scoring situation is $T_1 \succ T_3 \succ T_2$.
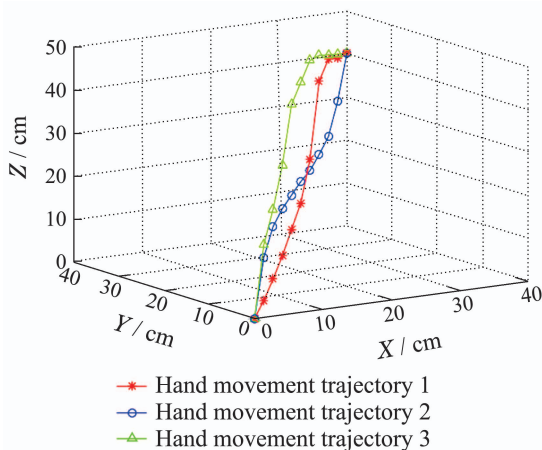

Fig. 4　Three trajectories from starting to target points

Taking the straight line as the reference line through the origin and the target point. Fig. 5 is a profile of Black line in Fig. 4 as reference line.

The P axis in Fig. 5 indicates the number of points in the trajectory, the Q axis indicates the distance between the point in the trajectory and the origin of the

coordinates. With the black line in the picture as a reference, in each track the Point records greater than reference values is 1, others value is 0. Among them, the passing point of T_2 can be expressed by [1, 1, 1, 1, 1, 0, 0, 0, 0], and T_1 can be expressed by [0, 0, 0, 0, 0, 0, 1, 1, 1], T_3 can be expressed by [1, 1, 1, 1, 1, 1, 1, 1, 1]. We can set up a data base [30] table with this manner, as shown in Table 1.
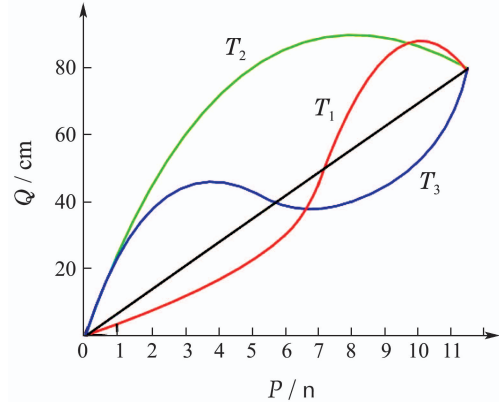

Fig. 5　Decomposition diagram with 11 points of three trajectories

The table is divided into two parts, in which the T_{gi} indicates a higher score, and the T_{bi} represents a lower one.

Table 1　Track data table D

Outcome	Tag	The serial number of pass point								
		P_1	P_2	P_3	P_4	P_5	P_6	P_7	P_8	P_9
O_{gi}	T_{g1}	0	0	0	0	0	0	1	1	1
	T_{g2}	0	0	0	0	0	1	1	1	1
	T_{g3}	1	1	1	1	1	1	1	1	1
O_{bi}	T_{b1}	1	1	1	1	1	1	1	1	1
	T_{b2}	1	1	1	1	1	0	0	0	0
	T_{b3}	1	1	1	1	0	0	0	0	0

3　Trajectory planning based on CP-nets

A conditional preference network (CP-net) N is a graph model G with the sets $\langle V, E, CPT \rangle$, in which:

$V = \{X_1, X_2, \cdots, X_n\}$ is a set of variables makes up the nodes in the network, and E is a set of directed edges connects pairs of nodes.

Each node has a conditional preference table $CPT(X_i)$ that qualifies the effects of its parents $Pa(X_i)$ on it.

In the CP-net, each $\text{Dom}(X_i)$ represents the finite definition domain of X_i. For each attribute X_i, the set of parent attributes $Pa(X_i)$ can affect the preferences over the values of X_i. This defines a dependency graph where each node X_i has an edge from each attribute in $Pa(X_i)$.

The graph G of CP-net does not define the structure. It may be either directed acyclic or directed cyclic. Our work mainly focuses on acyclic CP-net.

A preference database is expressed with $\{P, \langle O_{gi}, O_{bj} \rangle\}$. Let $P = (P_1, P_2, \cdots, P_9)$ be a preference schema with 9 attributes. The relation $\langle O_{gi}, O_{bj} \rangle$ denotes the fact that the user prefers outcome T_{gi} to T_{bj}.

Let $T(P_1, P_2, \cdots, P_9)$ be a preference schema with attribute domains given by $\text{Dom}(X) = \{x_0, x_1\}$ with $X = (P_1, P_2, \cdots, P_9)$, respectively. The preference relation is $O_{gi} \succ O_{bj}$. When the example is $T_{g1} \succ T_{b1}$, that is $[0, 0, 0, 0, 0, 0, 1, 1, 1] \succ [1, 1, 1, 1, 1, 1, 1, 1, 1]$, $T_{g2} \succ T_{b2}$, that is $[0, 0, 0, 0, 0, 0, 1, 1, 1] \succ [1, 1, 1, 1, 1, 0, 0, 0, 0]$.

In general, we take all samples into consideration. But some information may be useless, or can be regarded as noise data, the data can be used is called as evidence data. We give two thresholds to eliminate the data. For easy to understand, we give some concepts[31].

1) For each, $(P_m, P'_m) \in \text{dom}(P_m) \times \text{dom}(P_m)$, $P_m \neq P'_m$, O_{P_m, P'_m} is described as the subset of pairs $(P_m, P'_m) \in P$;

2) We present unconditional evidence as $E((P_m, P'_m), P) = \dfrac{|O_{P_m, P'_m}|}{|P|}$. The pair $(P_m, P'_m) \in \text{dom}(P_m) \times \text{dom}(P_m)$ is comparable if $E((P_m, P'_m), P) > \alpha_1$, of which α_1 is a threshold with $0 \leqslant \alpha_1 \leqslant 1$;

3) For each $P_n \in \text{dom}(P_n)$, $E_{P_n|(P_m, P'_m)}$ is described as the subset of O_{P_m, P'_m};

4) We present conditional evidence as

$$E(P_n|(P_m, P'_m), P) = \dfrac{|E_{P_n|(P_m, P'_m)}|}{\left| \bigcup\limits_{P_n \in \text{dom}(P_n)} E_{P_n|(P_m, P'_m)} \right|};$$

5) v is a factor for (P_m, P'_m) being comparable if $E(P_n \mid (P_m, P'_m), P) > \alpha_2$, of which α_2 is a threshold with $0 \leqslant \alpha_2 \leqslant 1$.

Given this, our algorithm builds a CP-nets structure using Algorithm 2.

Algorithm 2 (Learning CP-nets structure)
Input: the preference data D
For each pair (P_m, P_n), $P_m \neq P_n$, m and n from 1 to the last numbers of D.
Let $g_1(E_{P_n|(p_m, p'_m)}) = \max(N, 1 - N)$, where

$$N = \dfrac{|\{(o, o') \in (E_{P_n|(P_m, P'_m)}) : o > o' \wedge (o[P_m] = P'_m)\}|}{|E_{P_n|(P_m, P'_m)}|}$$

$g_2(O_{(P_m, P'_m)}) = \max\{g_1(E_{P_n|(P_m, P'_m)})\}$,
$g_3((P_m, P_n), P) = \max\{g_2(O_{(P_m, P'_m)})\}$

Order the $g_3(P_m, P_n)$ in decreasing order.
    For each $g_3(P_m, P_n)$, do
        If $g_3(P_m, P_n) > \alpha_2$, **then**
            Draw the dependencies $g_3 > \alpha_2$ in existence
            If one of $g_3(P_m, P_n)$ has created cycle
            then Remove the edge with lower g_3 in the cycle.
    End for
End for
Return CP-net
Output: A CP-net

According to the obtained CP-net and Data set D, we use algorithm 3 to obtain the CPT.

In Algorithm 3, if the attribute P_i does not have a $Pa(P_i)$, the preference of the statistical data set D is its preference; If P_i has a $Pa(P_i)$, the preference characteristic depends on the preference after combination, when the $Pa(P_i)$ chooses better values as conditions.

Algorithm 3 (Obtaining the CPT)
Input: The CP-net and Data set D
For P_i, i from 1 to 9
If $Pa(P_i) = \varnothing$
    For j from 1 to number of O_{gi}
        If $\text{Sum}(P_i = 0|T_{gi}) > \text{Sum}(P_i = 1|T_{bi})$
        The preference of $P_i = 0 \succ 1$
        If $\text{Sum}(P_i = 1|T_{gi}) > \text{Sum}(P_i = 0|T_{bi})$
        The preference of $P_i = 1 \succ 0$
    End for
If $Pa(P_i) \neq \varnothing$
    For $APa(P_i) = Pa(P_i)$ attribute values
        For j from 1 to number of O_{gi}
            If $\text{Sum}(P_i = 0|T_{gi} \&\& APa(P_i)) > \text{Sum}(P_i = 1|T_{bi} \&\& APa(P_i))$
            The preference of $P_i = 0 \succ 1$
            If $\text{Sum}(P_i = 1|T_{gi} \&\& APa(P_i)) > \text{Sum}(P_i = 0|T_{bi} \&\& APa(P_i))$
            The preference of $P_i = 1 \succ 0$
        End for
    End for
End for
Return CPT
Output: A CPT

4 Experiments and discussions

In this paper, the trajectory of the human hand is abstracted as a set of 11 points composed of 9 pass points, one starting point and one target point. According to the relative position of 9 passing points and reference trajectories, the values of points are divided into 0 and 1 two values. There are 2^9 different trajectories from a starting point to a fixed target. We collected 10 trajectories and arranged these trajectories according to the

score, generated preference database consisting of 45 comparisons. The CP-net obtained by this database as shown in Fig. 6.
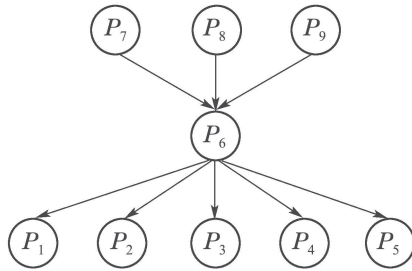

Fig. 6 The CP-net of pass points

The conditional preference table as shown in Table 2.

Table 2 Conditional preference table

Condition	Preference
/	$P_7 = 1 \succ P_7 = 0$
/	$P_8 = 1 \succ P_8 = 0$
/	$P_9 = 1 \succ P_9 = 0$
$P_7 = 1 \wedge P_8 = 1 \wedge P_9 = 1$	$P_6 = 1 \succ P_6 = 0$
$P_6 = 1$	$P_1 = 0 \succ P_1 = 1$
$P_6 = 1$	$P_2 = 0 \succ P_2 = 1$
$P_6 = 1$	$P_3 = 0 \succ P_3 = 1$
$P_6 = 1$	$P_4 = 0 \succ P_4 = 1$
$P_6 = 1$	$P_5 = 0 \succ P_5 = 1$

The optimal preference model for the trajectory of the human hand is as follows: [0, 0, 0, 0, 0, 1, 1, 1]. The trajectory is shown in Fig. 7.
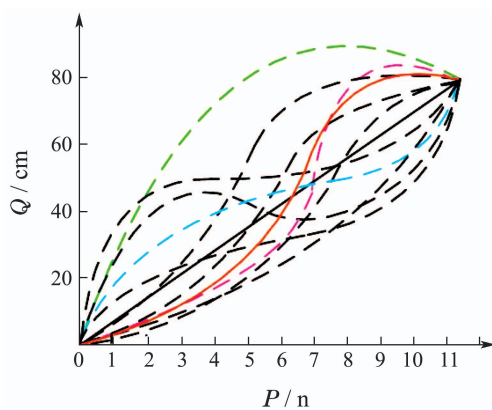

Fig. 7 Optimal trajectory based on CP-nets

The orange solid line in Fig. 7 is the optimal trajectory after the planning, and the remaining dashed line is the trajectory of the robot running according to the coordinates in the track data table. Our algorithm plans the optimal trajectory on a given track data table. According to the trajectory and the inverse solution algorithm of the robot, the control mode of the robot can be obtained.

The model moves the wrist in accordance with the trajectory coordinates of the solution, it indicates that the trajectory is more comfortable than others.

5 Conclusions and future work

The robot system is an extremely complex intelligent control system, and CP-nets is an important topic in the field of artificial intelligence. In this paper, we use CP-nets to study the trajectory of human arm, and then apply it to the robot arm to achieve the optimal trajectory control of robot. Because of the limited conditions, there are many problems need be further researched in future work, we will pay more attention to obtain optimal trajectory from multiple CP-nets[32]. Such problems would bring us closer to working with complex applications[33] in multi robots interaction.

References:

[1] CHANDRASEKARAN B, CONRAD J M. Human-robot collaboration: A survey [C] //*Proceedings of the Southeastcon*. Lauderdale: IEEE, 2015, 5: 1 – 8.

[2] ARAI T, KATO R. Assessment of operator stress induced by robot collaboration in assembly [J]. *CIRP Annals–Manufacturing Technology*, 2010, 59(1): 5 – 8.

[3] BRADLEY J, ABBOTT J. Microrobots for minimally invasive medicine [J]. *Annual Review of Biomedical Engineering*, 2010, 12(1): 10 – 55.

[4] ULLRICH F, BERGEIES C. Mobility experiments with microrobots for minimally invasive intraocular surgery [J]. *Investigative Ophthalmology & Visual Science*, 2013, 54(4): 2853 – 2864.

[5] AVANZINI G B, CERIANI N M, ZANCHETTIN A M. Safety control of industrial robots based on a distributed distance sensor [J]. *IEEE Transactions on Control Systems Technology*, 2014, 22(6): 2127 – 2140.

[6] AVANZINI G B, CERIANI N M, ZANCHETTIN A M. Optimal placement of spots in distributed proximity sensors for safe human-robot interaction [C] //*IEEE International Conference on Robotics and Automation*. Karlsruhe: IEEE, 2013: 5858 – 5863.

[7] DONG H, ZHONG X F, HUANG S. Trajectory planning method in joint space for 6-DOF robot [J]. *Journal of Zhejiang university of techonology*, 2015, 43(3): 336 – 339.

[8] MAHMOODI A, SAYADI A, MENHAJ M. Solution of forward kinematics in Stewart platform using six rotary sensors on joints of three legs [J]. *Advanced Robotics*, 2014, 28(1): 27 – 37.

[9] WANG Y, SHEN Y, GAI Y, et al. A robot kinematics simulation system based on OpenGL [C] //*IEEE 5th International Conference on Robotics, Automation and Mechatronics*. Qingdao: IEEE, 2011: 158 – 161.

[10] MOMI E D, KRANENDONK L, VALENTI M. A neural network-based approach for trajectory planning in robot chuman handover tasks [J]. *Frontiers in Robotics and AI*, 2016, 3(10): 34 – 43.

[11] HE W, DAVID A, YIN Z. Neural network control of a robotic manipulator with input deadzone and output constraint [J]. *IEEE Transactions on Systems Man and Cybernetics Systems*, 2016, 46(6): 759 – 770.

[12] HE W, CHEN Y. Adaptive neural network control of an uncertain robot with full-state constraints [J]. *IEEE Transactions on Cybernetics*, 2016, 46(3): 620 – 629.

[13] SMISEK J, JANCOSEK M, PAJDLA T. 3D with kinect [C] //*IEEE International Conference on Computer Vision Workshops*. Barcelona: IEEE, 2011: 1154 – 1160.

[14] HUANG R, CHENG H, CHEN Y. Optimisation of reference gait trajectory of a lower limb exoskeleton [J]. *International Journal of Social Robotics*, 2016, 8(2): 223 – 235.

[15] JATESIKTAT P, WEI A. Recovery of forearm occluded trajectory in Kinect using a wrist-mounted inertial measurement unit [C] //*International Conference of the IEEE Engineering in Medicine and Biology Society*. Barcelona: IEEE, 2017: 807 – 812.

[16] GUO X, YANG T. Gesture recognition based on HMM-FNN model using a kinect. *Journal on Multimodal User Interfaces*, 2016, 11(1): 1 – 7.

[17] BOUTILIER C, BRAFMAN R I, DOMSHLAK C. CP-nets: a tool for representing and reasoning with conditional ceteris paribus preference statements [J]. *Journal of Artificial Intelligence Research*, 2004, 21(1): 135 – 191.

[18] OHISHI K, MAJIMA K, FUKUNAG T. Gait control of biped robot based on kinematics and motion description in cartesian space [J]. *Electrical Engineering in Japan*, 2015, 129(4): 96 – 104.

[19] MIYASHITA D, KOUSAI S. A neuromorphic chip optimized for deep learning and cmos technology with time-domain analog and digital mixed-signal processing [J]. *IEEE Journal of Solid-State Circuits*, 2017, 52(10): 2679 – 2689.

[20] ANGE N, KARL F, GIOVANNI P. Active inference and robot control: a case study [J]. *Journal of the Royal Society Interface*, 2016, 13(122): 1 – 12.

[21] GAO Z, YU Y, ZHOU Y. Leveraging two kinect sensors for accurate full-body motion captur [J]. *Sensors*, 2015, 15(9): 24297 – 24317.

[22] CALLEGARI S, ROVATT R, SETTI G. Embeddable ADC-based true random number generator for cryptographic applications exploiting nonlinear signal processing and chaos [J]. *IEEE Transactions on Signal Processing*, 2005, 53(2): 793 – 805.

[23] MARTINEC T, MLYNEC J, PETU M. Calculation of the robot trajectory for the optimum directional orientation of fibre placement in the manufacture of composite profile frames [J]. *Journal of Biological Chemistry*, 2015, 35(15): 42 – 54.

[24] REZAEIAN J, GHAEMI O, ALI M. Optimization of kinematic redundancy and workspace analysis of a dual-arm cam-lock robot [J]. *Robotica*, 2016, 34(1): 23 – 42.

[25] MAJEWICZ A, OKAMURA T. Cartesian and joint space teleoperation for nonholonomic steerable needles [C] //*World Haptics Conference*. Chicago: IEEE, 2013: 395 – 400.

[26] XU W, LIANG B, LI C. Path Planning of Free-Floating Robot in Cartesian Space Using Direct Kinematics [J]. *International Journal of Advanced Robotic Systems*, 2008, 4(12): 17 – 27.

[27] ASFOUR T, DILLMANN R. Human-like motion of a humanoid robot arm based on a closed-form solution of the inverse kinematics problem [C] //*IEEE/RSJ International Conference on Intelligent Robots and Systems*. Hamburg: IEEE, 2003, 2: 1407 – 1412.

[28] ROCHA R, TONETTO C, DIAS A. A comparison between the Denavit CHartenberg and the screw-based methods used in kinematic modeling of robot manipulators [J]. *Robotics and Computer-Integrated Manufacturing*, 2011, 27(4): 723 – 728.

[29] SAOTA A. An algorithm for generation of coordinated robot trajectories in cartesian space [J]. *Solid State Phenomena*, 2013, 196: 169 – 180.

[30] LIU Z, ZHONG Z, LI K, et al. Structure learning of conditional preference networks based on dependent degree of attributes from preference database [J]. *IEEE Access*, 2018, 6(1): 27864 – 27872.

[31] AMO S De, DIALLO M S, DIOP C T, et al. Contextual preference mining for user profile construction [J]. *Information Systems*, 2015, 49: 182 – 199.

[32] LI M, KOWALCZYK R. Aggregating multi-valued CP-nets: a CSP-based approach [J]. *Journal of Heuristics*, 2015, 21(1): 1 – 34.

[33] OU L L, CHEN H, XIAO Y T, et al. Design and implement of optimal patrolling control system to satisfy the complex requirements [J]. *Control Theory & Applications*, 2016, 33(2): 172 – 180.

作者简介:

    刘兆伟 (1979–), 男, 副教授, 博士研究生, 主要研究方向为智能控制、多agent系统和机器学习等, E-mail: liu.zhaowei@163.com;

    仲兆琳 (1993–), 男, 硕士研究生, 主要研究方向为人工智能领域的CP-nets研究等, E-mail: ytdxzzl@sina.com;

    王　磊 (1991–), 男, 硕士, 主要研究方向为机器人控制, E-mail: ytuwanglei@sina.com;

    李　珂 (1979–), 男, 副教授, 博士, 主要研究方向为可再生能源、储能技术、电力电子和运动控制, E-mail: like@sdu.edu.cn.